DOI: 10.4408/IJEGE.2018-01.S-05

FUTURE PRECIPITATION AND TEMPERATURE CHANGES OVER THE TARO, PARMA AND ENZA RIVER BASINS IN NORTHERN ITALY

Marco D'ORIA, Chiara COZZI & Maria Giovanna TANDA

University of Parma - Department of Engineering and Architecture - Parco Area delle Scienze, 181/A - 43124 Parma, Italy
Corresponding author: mariagiovanna.tanda@unipr.it

EXTENDED ABSTRACT

I cambiamenti climatici rappresentano un fenomeno attuale e molto discusso anche dal punto di vista politico: sono stati rilevati aumenti delle temperature, alterazioni dei regimi pluviometrici, scioglimento di ghiacciai e nevai, e il livello medio del mare è in aumento. Si prevede che tali cambiamenti continueranno e che gli eventi climatici estremi all'origine di pericoli quali alluvioni e siccità diventeranno sempre più frequenti ed intensi. Secondo la maggior parte della comunità scientifica internazionale, molte delle alterazioni verificatesi nell'ultimo secolo sono sostanzialmente dovute all'osservato aumento delle concentrazioni di gas ad effetto serra. Sebbene il cambiamento climatico sia globale, i suoi impatti spesso variano da regione a regione. I principali strumenti disponibili ai ricercatori per analizzare il clima futuro sono basati sulle proiezioni dei modelli di circolazione generale (GCM) e dei modelli climatici regionali (RCM) che forniscono le variabili climatiche di interesse (ad esempio precipitazione e temperatura) su una griglia che include l'intero globo (GCM) o una porzione di esso (RCM). Tali modelli hanno l'obiettivo di descrivere i cambiamenti climatici a lungo termine simulando i processi che avvengono nel sistema atmosferico, negli oceani e sulla superficie terrestre, a livello globale o regionale. Parametri, quali ad esempio la concentrazione di gas ad effetto serra in atmosfera, costituiscono le forzanti in ingresso.

Il primo obiettivo di questo studio è quello di analizzare le eventuali future variazioni della precipitazione e della temperatura, nel quadro dei cambiamenti climatici, con riferimento ai bacini idrografici del fiume Taro e dei torrenti Parma ed Enza, in Emilia Romagna. A tal fine, si è utilizzato un insieme di 13 modelli climatici regionali (RCM) sviluppati in seno al progetto EURO-CORDEX secondo due differenti scenari di emissione di agenti forzanti: lo scenario denominato RCP 4.5 e lo RCP 8.5. Per questa tipologia di studi, l'utilizzo di un insieme di modelli climatici si rende necessario al fine di caratterizzare e quantificare l'incertezza insita nelle proiezioni future. I risultati di questa analisi sono presentati in termini di "anomalie" tra la precipitazione e la temperatura media valutate in un periodo di riferimento (RP, 1986-2005) e quelle di tre periodi futuri: uno a breve (ST) 2016-2035, uno a medio (MT) 2046-2065 e uno a lungo termine (LT) 2081-2100. Con lo scopo di confrontare i risultati, le anomalie sono state valutate considerando sia i dati grezzi provenienti dagli RCM che quelli corretti dagli errori sistematici in essi presenti (bias correction) sulla base di osservazioni storiche disponibili sull'area di studio. Le analisi sono state condotte sia a scala stagionale che a scala annuale. Con riferimento alle precipitazioni, le variazioni nei tre periodi futuri risultano irregolari e spesso moderate; a scala annuale e sulla base del valore mediano dei 13 modelli climatici, deviazioni comprese tra -5% e +6% si alternano nei vari periodi e per i due scenari. Le variazioni tra i vari modelli risultano elevate mettendo in evidenza l'ampio grado di incertezza dei risultati. Per quanto riguarda le temperature, invece, il graduale riscaldamento dell'area di studio, nell'arco dei tre periodi futuri analizzati, appare inequivocabile. Sempre con riferimento al valore mediano dei modelli climatici e alla scala annuale, si stimano incrementi di temperature fino a +0.75°C a ST, +1.5°C a MT e +2°C a LT, per lo scenario RCP 4.5. Gli incrementi raggiungono +1°C a ST, +2°C a MT e +4°C a LT secondo lo scenario 8.5. Sebbene l'aumento delle temperature sia indubbio, anche in questo caso i risultati mostrano un'elevata variabilità tra i 13 modelli climatici; l'effetto della correzione del bias presente nelle proiezioni dei modelli RCM risulta in una diminuzione della loro variabilità.

In questo studio, alle variazioni della precipitazione e temperatura, si è affiancata un'analisi utile a determinare e a quantificare la presenza di trend nelle variabili climatiche future, sempre sulla base delle proiezioni dei modelli RCM. A tale scopo si sono utilizzati il test non parametrico di Mann-Kendall e lo stimatore di Theil Sen. L'evoluzione nel tempo dei trend di precipitazione e temperatura, sull'area di studio, è stata analizzata nel periodo 1976-2100 e con riferimento a una finestra mobile di ampiezza 30 anni, sempre a scala stagionale ed annuale. Quest'analisi ha confermato i risultati precedenti: trend non significativi e poco robusti per quanto riguarda le precipitazioni e al contrario trend positivi e in accordo tra i vari modelli per quanto riguarda le temperature. I risultati hanno anche messo in evidenza, specialmente per i dati di temperatura, l'esistenza di uno stretto legame tra l'evoluzione nel tempo dei trend e gli scenari di emissione esaminati.

La variabilità dei risultati ottenuti in questo studio, giustifica l'utilizzo di un ricco insieme di modelli climatici regionali che permettono di tenere in considerazione l'incertezza delle proiezioni future; l'uso di un singolo modello climatico può infatti portare a conclusioni non complete e fuorvianti.

ABSTRACT

This study analyzes the climate change effects on the future precipitation and temperature over the Taro, Parma and Enza River basins, in the Emilia Romagna region, northern Italy. An ensemble of 13 Regional Climate Models and two emission scenarios (RCP 4.5 and RCP 8.5) were adopted. The results are reported in terms of precipitation and mean temperature anomalies between a reference period (RP, 1986-2005) and three future periods: short-term (ST) 2016-2035, medium-term (MT) 2046-2065 and long-term (LT) 2081-2100. With reference to the rainfall data, irregular and slight variations are expected at any season and period; on a yearly scale, changes from -5% to +6% are estimated. On the other hand, a gradual warming of the study domain in the future periods is unequivocal. At annual scale, increments up to +0.75°C at ST, +1.5°C at MT and +2°C at LT are expected under the RCP 4.5, and higher, up to +4°C at LT with the RCP 8.5. In addition, the trend evolution of the climate variables was analyzed using a thirty-year moving time window up to the end of the century. From the results, it is evident that the pattern of the trend gradients follows the pattern of the scenario radiative forcing.

Keywords: *climate change, climate model, precipitation trend, temperature trend*

INTRODUCTION

Climate change is one of the most debated issues from a scientific and political point of view (IPCC, 2014). Although climate change occurred at a global scale, its impact often varies from region to region. The main tools available to the research community to analyze future climate are the General Circulation Model (GCM) and the Regional Climate Model (RCM) projections, which provide climatic variables of interest (e.g. precipitation and temperature) on a grid that includes the whole globe (GCMs) or only a portion of it (RCMs). The aim of these models is to describe the long-term climate changes by simulating the processes occurring in the atmospheric system, in the oceans and on the Earth's surface, at global or regional level. Parameters such as the concentrations of greenhouse gases within the atmosphere are the model forcing inputs. Although GCMs are based on defined physical principles and are able to simulate the average features of climate, their outputs have a low spatial resolution. GCM grids have a horizontal resolution between 100 and 600 km, which makes their use unsuitable for local or basin scale impact assessments; for this reason, Regional Climate Models are preferred. Each RCM is coupled to a specific GCM, which provides its boundary conditions, producing finer resolution data (10-50 km). However, uncertainty exists in all climate simulations and the most relevant sources are: (I) the selection of the greenhouse gas emission scenario; (II) the choice of the GCM model. Even using the same scenarios and boundary conditions, different global models use different schemas in solving the basic equations and hence come to different results; (III) the RCM choice. For these reasons, it is recommended to use the results of an ensemble of climate models (combinations of GCMs and RCMs) and plausible forcing scenarios; in this way, it is possible to characterize and deal with the uncertainty in the results (Sulis *et alii*, 2012; Teutschbein & Seibert, 2012).

Over the last decades, on European scale, several projects have been founded to make available regional projections of the future climate (RCM data). Among them, the ENSEMBLES project (Van Der Linden & Mitchell, 2009), provides data from 1951 to 2100 using 15 different RCMs with a spatial resolution of 25 km. The data were generated according to different scenarios based on the Intergovernmental Panel on Climate Change (IPCC) Special Report on Emissions Scenarios (SRES, Nakicenovic *et alii*, 2000).

Subsequent to the ENSEMBLES project, the initiative coordinated by the World Climate Research Program (WCRP), called CORDEX (Giorgi *et alii*, 2009) provides global projections up to 2100 at a spatial resolution ranging from about 12.5 km (0.11°, grid EUR-11) to 50 km (0.44°, grid EUR-44). These models account for the greenhouse gas forcing adopting the scenarios named Representative Concentration Pathways (RCPs) assumed by the IPCC in the Fifth Assessment Report (AR5, IPCC, 2014). Within the CORDEX project, the area of interest for this study is included into the EURO-CORDEX branch (Jacob *et alii*, 2014), which is focused on defining climate projections in Europe to better understand the regional climate phenomena and their variability.

The first aim of this study is the analysis of future precipitation and temperature changes over the Taro River, Parma River and Enza River basins, in the Emilia Romagna region, northern Italy. Vezzoli *et alii* (2015) analyzed the effect of future climate changes on the Po River basin (that includes our study area) in two future periods (2041-2070 and 2071-2100), under the RCP4.5 and RCP8.5 scenarios; the Authors used only one RCM model. The Authors found that precipitation is expected to decrease in spring and summer and increase in fall (under the RCP4.5 only) and winter, while temperatures is expected to increase in all seasons. In this paper, we used an ensemble of 13 RCMs, in order to take account of the uncertainty and of the variability of the projections, and we focus on a smaller area. It is established, in literature, that climate models projections are affected by systematic errors (Gudmundsson *et alii*, 2012; Teutschbein & Seibert, 2012, 2013; Chen *et alii*, 2013) and therefore a correction is needed, especially for hydrologic impact studies. Teutschbein & Seibert (2012) reviewed different downscaling/bias correction methods; in this study we used the Distribution Mapping method that appears to outperform the other. We also compared the results obtained by means of the raw RCM data and the downscaled/bias corrected ones.

The second purpose of this study is to detect and quantify the presence of trends in the future climate variables as projected by

the different models. At this aim we adopted the Mann-Kendall test (Mann, 1945, Kendall, 1955), one of the widely used non-parametric tests (Hamed & Rao, 1998), and the Theil Sen slope estimator (Sen, 1968). The assessment of future trends in climate time series is not new in literature; see for example Semiromi *et alii* (2014), Razavi *et alii* (2016). In this study, differently from other authors, we analyzed the evolution of the precipitation and temperature trend over the study area in the period 1976-2100, using a mobile time window of thirty years.

This paper is organized as follows. First the study area and the available dataset are described. Then, the methods used in the analysis of the future climate projections (with bias-corrected and raw data) and of future trends are outlined. After the presentation of the results, conclusions are finally drawn.

STUDY AREA AND DATASETS

The study area covers the entire territory of the province of Parma and a small portion of the province of Reggio Emilia; it is located on the western part of the Emilia Romagna region, in northern Italy. The Taro River, Parma River and Enza River basins are within the area (Fig. 1). The study domain has an area of about 3,700 km^2, 65% of which is located in mountain areas. Its elevation varies between 50 m a.s.l. and 2000 m a.s.l. from northeast to southwest. The annual mean precipitation is between 800 mm (in the plain) and 2000 mm (in the mountains), while the average temperature ranges approximately between -1.3°C (January) and +24.4°C (July).

Despite many rain and temperature gauges are distributed throughout the territory, in the period 1976-2005 (used as control period in the following analyses), only 26 precipitation and 5 temperature stations have observed data recorded with a tolerable number of missing data (we set in 70% the minimum percentage of available data). Figure 1 shows the location of the weather stations and Table 1 reports the gauge characteristics and the percentage of available data; for these stations, precipitation and temperature records are available at daily scale.

To assess future precipitation and temperature over the study area, we made use of a multi-model ensemble of GCM and RCM projections. In fact, as already pointed out, it is recommended to use and compare the results of different climate models, forced by different emission scenarios, to obtain a more realistic assessment of the future climate and to account for the uncertainty (D'Oria *et alii*, 2017). For this reason, we used the data of 13 combinations of GCMs and RCMs (Tab. 2) provided by the EURO-CORDEX project (Jacob *et alii*, 2014). We selected the available models with the finer spatial resolution (grid EUR-11): 0.11°, corresponding to a grid size of about 12.5 km; Fig. 1 shows the portion of the grid covering the study area. Two different emission scenarios, RCP

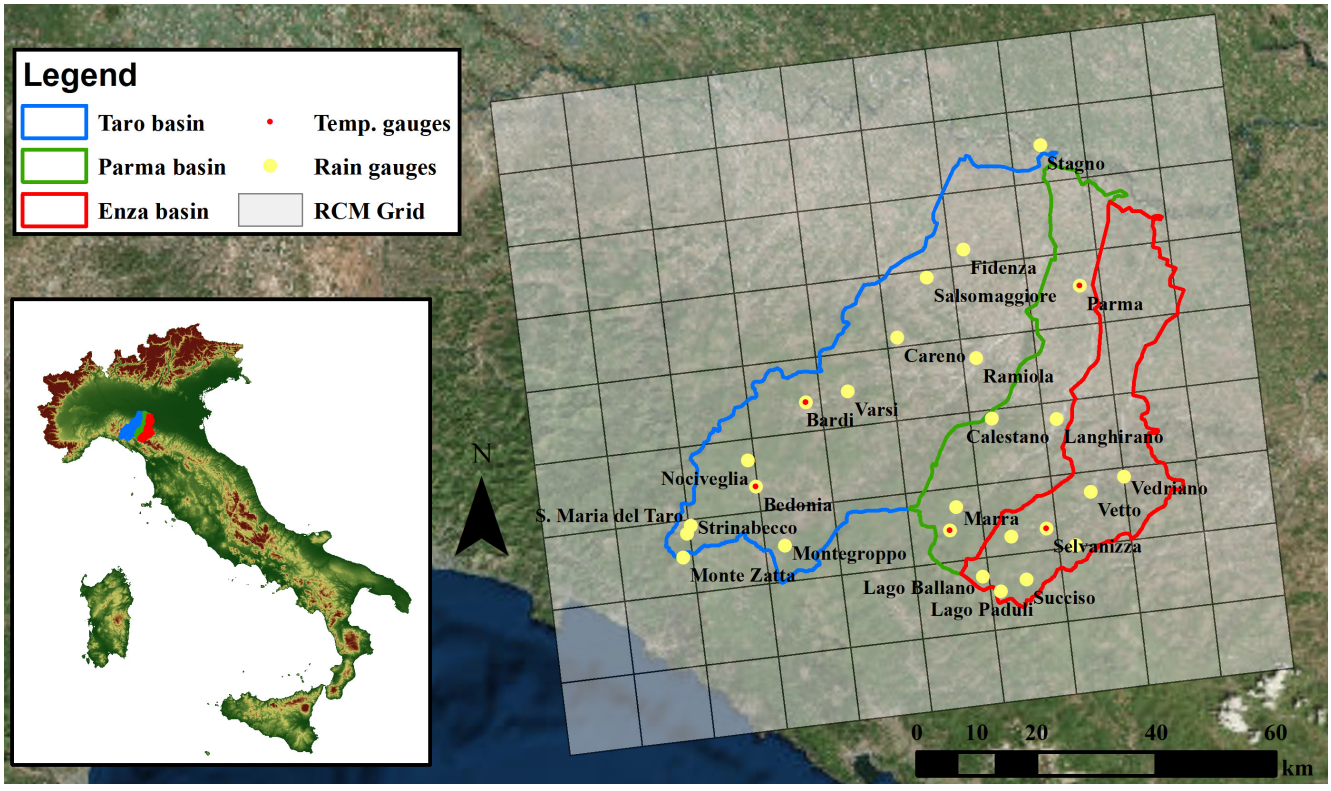

Fig. 1 - Study area, rain and temperature gauges used in this study and portion of the EUR-11 RCM grid

Station name	Altitude (m a.s.l.)	Available precipitation data Period 1976-2005 (%)	Available temperature data Period 1976-2005 (%)
Bardi	430	94.9	86.1
Bedonia	544	100	97.2
Bosco di Corniglio	784	80.6	91.7
Calestano	417	94.4	
Canova di Ramiseto	790	80.6	
Careno	581	88.9	
Fidenza	75	91.7	
Isola di Palanzano	575	86.1	
Lago Ballano	1335	69.4	
Lago Paduli	1139	100	
Langhirano	262	75.0	
Marra	635	88.9	
Monte Zatta	1125	83.3	
Montegroppo	800	83.3	
Nociveglia	855	72.2	
Parma	55	100	91.7
Ramiola	145	86.1	
S. Maria del Taro	744	77.8	
Salsomaggiore	160	88.9	
Selvanizza	468	88.9	94.4
Stagno	32	72.2	
Strinabecco	800	91.7	
Succiso	911	86.1	
Varsi	315	83.3	
Vedriano	590	75.0	
Vetto	437	86.1	

Tab. 1 - Gauging station characteristics and percentage of available precipitation and mean temperature daily data in the period 1976-2005

4.5 and RCP 8.5, were adopted. Precipitation and temperature data are available at daily scale for each grid element for the period 1950/1970-2100; the climate model projections originate from a historical simulation until 2005 (hindcast period) and scenario runs in the period 2006-2100.

For the following analysis, seasonal and annual data, for both the instrumental and the climate models time series, have been calculated as cumulative precipitation and mean temperature in the selected periods. We considered winter to be the months of December, January and February (DJF), spring as March, April and May (MAM), summer as June, July and August (JJA) and fall as September, October and November (SON).

METHODS

Future climate model projections

In order to assess the effects of climate change over the study area, we used the available RCM data to evaluate the precipitation and mean temperature anomalies (variations between the future projections and the data in a historical reference interval) in selected future periods.

As already pointed out, the variables obtained by means of climate models are often affected by systematic errors and can be not representative for the local climate, because of the imperfect model conceptualization, the discretization and spatial averaging within grid cells (Teutschbein & Seibert, 2010). For these reasons, a downscaling/bias correction technique can be applied to the raw RCM data before using them for climate assessment studies. Different methods can be used to correct the raw RCM outputs; a comprehensive review is available in Teutschbein & Seibert (2012). In this study, we used the Distribution Mapping method (also known as quantile-quantile-mapping, Teutschbein & Seibert, 2012), that in comparison with other methodologies, is often indicated as the most effective in correcting precipitation and temperature data (Gudmundsson *et alii*, 2012; Teutschbein & Seibert, 2012, 2013;

		GCM				
		CNRM-CM5	EC-EARTH	HadGEM2-ES	MPI-ESM-LR	IPSL-CM5A-MR
RCM	CCLM4-8-17	X	X	X	X	
	HIRHAM5		X			
	WRF331F					X
	RACMO22E		X	X		
	RCA4	X	X	X	X	X

Tab. 2 - GCM and RCM combinations, used in this study, available from the EURO-CORDEX project. More information is available at www.euro-cordex.net

Chen *et alii*, 2013). The objective of this method is to match, in a chosen control period (when both observed and climate model daily data are available), the cumulative distribution function of the RCM-simulated climate variables and of the observed ones. The transfer function identified for the control period is then applied for the scenario projections (Teutschbein & Seibert, 2013). The correction was made on a monthly scale (i.e. for each monthly separately) adjusting, at gauging station scale, the daily time series obtained interpolating the raw RCM data at each observation site (downscaling). At this aim, we used an interpolation procedure based on the data available at the nine nearest RCM grid centers of gravity to the considered station and applying an inverse distance (power of 2) method.

Different distribution functions were used to model the hydrological variables: the Gamma distribution was adopted to characterize the wet-day precipitation time series, while the Gaussian distribution was assumed to fit the temperature ones. In correcting the rainfall data, a prior adjustment of the wet-day frequencies of the RCM data was applied to match the number of observed and modeled rainy days (see e.g. Teutschbein & Seibert, 2012, D'Oria *et alii*, 2017).

The precipitation and temperature anomalies were calculated using both the raw RCM data and the bias corrected ones. The data at station scale were then used to estimate the mean climate variables over the study area using the Thiessen polygon method.

We are aware that, if the RCM errors are merely systematic, the results in terms of anomalies should not be affected. However, since the downscaling/bias correction method used in this study is not just a linear transformation, we made the attempt to compare the results.

Future seasonal and annual trends

In addition to the evaluation of the future precipitation and temperature anomalies, we used the RCM data to detect seasonal and annual trends in the climate variables. In order to identify and quantify trends in the precipitation and temperature time series, the Mann-Kendall (MK) test (Mann, 1945, Kendall, 1955) and the method of Theil-Sen (TS, Sen, 1968) were used, respectively.

The Mann-Kendall test is a non-parametric statistical test that does not include specific hypothesis on the data distribution. It is widely applied to detect the presence of monotonic trends in hydrological time series (Yue & Pilon, 2004, Hamed, 2008, Nalley *et alii*, 2012, Razavi *et alii*, 2016, Chattopadhyay & Edwards, 2016). The null hypothesis (*H*) assumes that the data are independent and identically distributed (absence of trend), and this is tested against the alternative hypothesis of presence of trend. Given a series of observations x_i, with $t = 1, ..., N$, one compares the pairs of data (x_i, x_j) with $j>i$, and j belonging to the interval $[1, N]$. The formulation of the test statistic is:

$$S = \sum_{i=1}^{N-1} \sum_{j=1+1}^{N} \operatorname{sgn}(x_j - x_i)$$

where $sgn(x_j-x_i)=1$ if $x_j>x_i$, $sgn(x_j-x_i)=-1$ if $x_j<x_i$ and 0 otherwise. In practice, it is better to conduct the test through the parameter:

$$Z = \begin{cases} \dfrac{S-1}{\sqrt{V(S)}} & \text{per } S > 0 \\ 0 & \text{per } S = 0 \\ \dfrac{S+1}{\sqrt{V(S)}} & \text{per } S < 0 \end{cases}$$

where V(S) is the variance of S under the assumption of independent and identically distributed data:

$$V(S) = \frac{N(N-1)(2N+5)}{18}$$

When there are tied ranks in the data (equal values), V(S) is adjusted and becomes (Hamed, 2008):

$$V(S) = \frac{1}{18}\left(N(N-1)(2N+5) - \sum_{j=1}^{m} t_j(t_j-1)(2t_j+5)\right)$$

where m is the number of groups of tied ranks, each with t_j tied observations.

The Z function is preferable to the parameter S since it has a standard normal distribution and hence it allows to easily obtain the probability values (p-values). The null hypothesis is rejected (and the alternative hypothesis of presence of trend accepted) if *Z* has a *p*-value less than the chosen level of significance. The MK test is based on the assumption that the data are independent of each other, that means they do not present serial-correlation, otherwise, the outcome of the significance test is influenced. To solve this problem, Hamed & Rao (1998) developed a correction factor that modifies the variance of the MK statistic to compensate correlation effect. The correction is evaluated according to the coefficients of auto-correlation of the ranks of data. As reported by Hamed & Rao (1998) these coefficients must be calculated after applying a de-trend procedure to the data. We used this correction in the present work.

To quantify (linear) trends in the data, the TS slope estimator (Sen, 1968) was used. It is a non-parametric method and is less sensitive to outliers than the simple linear regression model. Given *N* couples of data x_i and y_i, according to the TS method, the slope of the trend line is calculated as the median of all the slopes $\frac{(y_j-y_i)}{(x_j-x_i)}$ (con $x_j>x_i$) that can be calculated for each pair of points belonging to the data set.

RESULTS

Future climate model projections

To investigate the effect of climate change over the study area, we evaluated the precipitation and mean temperature

		RCP 4.5 - Corrected data - Rainfall Anomaly [-]					RCP 4.5 - Raw data - Rainfall Anomaly [-]				
		Winter	Spring	Summer	Fall	Year	Winter	Spring	Summer	Fall	Year
2016-2035	Min	0.91	0.82	0.85	0.86	0.91	0.89	0.83	0.84	0.85	0.91
	25° perc	1.00	0.93	0.91	0.94	0.99	0.98	0.92	0.97	0.94	0.97
	Median	1.08	0.97	1.02	0.98	1.02	1.04	0.96	0.99	0.97	1.00
	75° perc	1.12	1.02	1.08	1.15	1.06	1.11	1.00	1.04	1.10	1.02
	Max	1.30	1.19	1.42	1.26	1.13	1.20	1.13	1.14	1.19	1.07
2046-2065	Min	0.94	0.73	0.54	0.79	0.84	0.94	0.74	0.60	0.80	0.86
	25° perc	1.02	0.92	0.77	0.94	0.95	0.99	0.91	0.83	0.92	0.94
	Median	1.04	0.96	0.90	0.98	1.00	1.00	0.94	0.86	0.95	0.96
	75° perc	1.14	0.99	0.98	1.17	1.04	1.11	0.97	0.91	1.13	1.00
	Max	1.25	1.16	1.11	1.23	1.08	1.24	1.15	1.03	1.21	1.04
2081-2100	Min	1.05	0.81	0.78	0.91	0.92	1.00	0.80	0.80	0.89	0.90
	25° perc	1.11	0.88	0.84	0.95	1.00	1.06	0.86	0.87	0.94	0.99
	Median	1.17	0.99	1.00	1.04	1.06	1.10	0.97	0.95	1.00	1.01
	75° perc	1.29	1.04	1.18	1.08	1.10	1.23	1.00	1.04	1.05	1.05
	Max	1.44	1.13	1.50	1.28	1.22	1.32	1.07	1.19	1.17	1.12

Tab. 3 - Seasonal and annual rainfall anomalies between the reference period (RP, 1986-2005) and the short (ST, 2016-2035), medium (MT, 2046-2065) and long (LT, 2081-2100) term periods, according to the RCP 4.5 scenario and both the downscaled/bias corrected and raw RCM data. The anomalies represent the ratios between the future projections and the RP data

anomalies between a reference period (RP, 1986-2005) and three future periods (according to the AR5, IPCC, 2014): short-term (ST) 2016-2035, medium-term (MT) 2046-2065 and long-term (LT) 2081-2100. All the analyses are based on the ensemble of 13 RCM projections provided by the EURO-CORDEX project under both the RCP4.5 and the RCP8.5 scenarios. As already pointed out, for comparison, the anomalies were calculated using both the raw RCM data and the downscaled/bias corrected ones. The correction factors were identified in the control period 1976-2005 (30 years) in which, in addition to the RCM data, observations were available for 26 rain and 5 temperature gauges. We are aware that the number of stations and their spatial distribution can be inadequate to capture the local climate, and for this reason the results focus on the entire study area and are expressed in terms of anomalies instead of absolute values. The analyses are performed at seasonal and annual scale.

With reference to the rainfall data, Table 3 reports the anomalies, obtained using corrected and raw RCM data under the RCP 4.5 scenario, between the reference period (RP) and each future period (ST, MT and LT) at seasonal and annual scale. In particular, the table reports the first three quartile of the RCM ensemble distribution and the minimum and maximum values. The precipitation anomalies represent the ratios between the future projections and the RP data: values greater than 1 indicate an increase in rainfall (e.g., 1.02 express an increase of 2%), while values smaller than 1 show a decrease (e.g., the value 0.97 indicate a decrease of 3%). The results

		RCP 8.5 - Corrected data - Rainfall Anomaly [-]					RCP 8.5 - Raw data - Rainfall Anomaly [-]				
		Winter	Spring	Summer	Fall	Year	Winter	Spring	Summer	Fall	Year
2016-2035	Min	0.89	0.79	0.67	0.87	0.96	0.87	0.80	0.71	0.86	0.94
	25° perc	0.96	0.99	0.94	0.98	0.99	0.96	0.96	0.91	0.95	0.98
	Median	1.03	1.04	1.02	1.02	1.04	1.00	1.02	0.97	1.03	0.99
	75° perc	1.10	1.13	1.16	1.17	1.09	1.07	1.06	1.07	1.11	1.03
	Max	1.21	1.25	1.39	1.31	1.15	1.18	1.21	1.12	1.22	1.11
2046-2065	Min	0.94	0.73	0.73	0.95	0.96	0.93	0.74	0.75	0.91	0.94
	25° perc	1.01	0.91	0.85	1.00	1.03	0.98	0.90	0.87	0.98	0.98
	Median	1.06	0.98	0.97	1.10	1.06	1.03	0.96	0.94	1.03	0.99
	75° perc	1.18	1.08	1.16	1.17	1.08	1.07	1.02	1.08	1.11	1.02
	Max	1.32	1.10	1.50	1.28	1.17	1.19	1.07	1.15	1.24	1.07
2081-2100	Min	0.85	0.74	0.45	0.91	0.88	0.80	0.73	0.52	0.86	0.86
	25° perc	1.06	0.85	0.55	0.96	0.92	0.99	0.85	0.62	0.95	0.90
	Median	1.14	0.90	0.70	1.02	0.99	1.10	0.87	0.69	0.97	0.95
	75° perc	1.23	1.01	0.80	1.17	1.04	1.17	0.95	0.80	1.11	0.98
	Max	1.31	1.15	1.59	1.23	1.29	1.27	1.13	1.25	1.19	1.10

Tab. 4 - Seasonal and annual rainfall anomalies between the reference period (RP, 1986-2005) and the short (ST, 2016-2035), medium (MT, 2046-2065) and long (LT, 2081-2100) term periods, according to the RCP 8.5 scenario and both the downscaled/bias corrected and raw RCM data. The anomalies represent the ratios between the future projections and the RP data

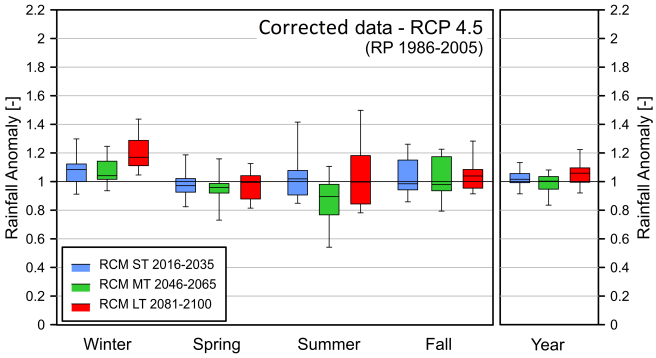

Fig. 2 - Box-whisker plots of the rainfall anomalies using the downscaled/bias corrected RCM data at ST, MT and LT, according to the RCP 4.5 scenario. The whiskers extend to the minimum and maximum values

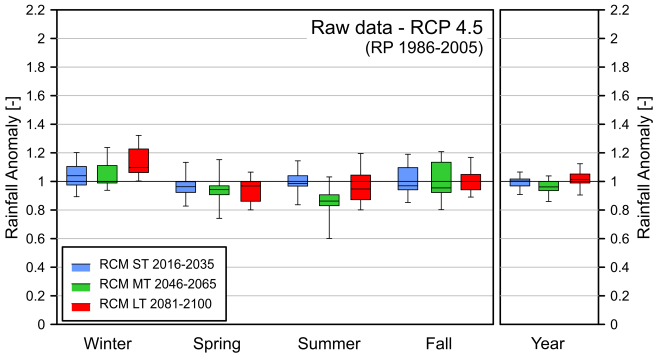

Fig. 3 - Box-whisker plots of the rainfall anomalies using the raw RCM data at ST, MT and LT, according to the RCP 4.5 scenario. The whiskers extend to the minimum and maximum values

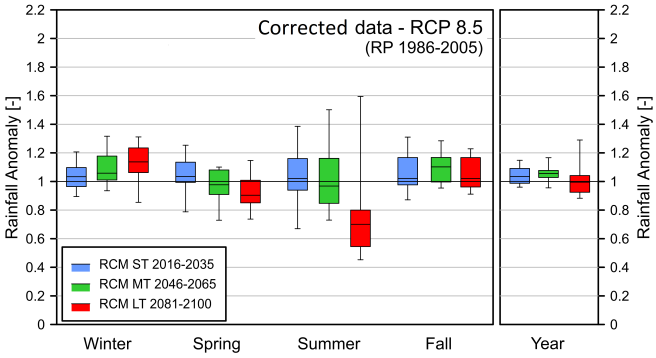

Fig. 4 - Box-whisker plots of the rainfall anomalies using the downscaled/bias corrected RCM data at ST, MT and LT, according to the RCP 8.5 scenario. The whiskers extend to the minimum and maximum values

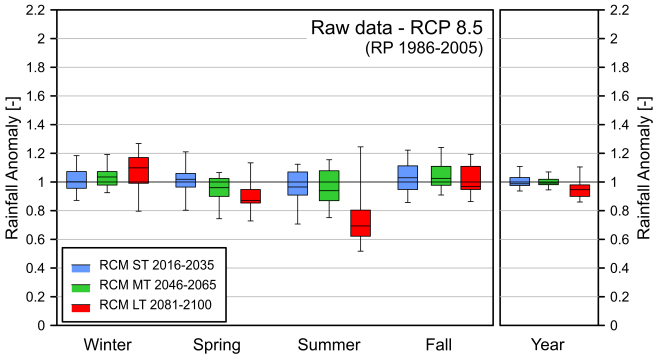

Fig. 5 - Box-whisker plots of the rainfall anomalies using the raw RCM data at ST, MT and LT, according to the RCP 8.5 scenario. The whiskers extend to the minimum and maximum values

show irregular and slight variations throughout any season using both the corrected and raw data. This is also highlighted in Fig. 2 (corrected data) and Fig. 3 (raw data) that show the results in terms of box-whisker plots (the whiskers extend to the maximum and minimum values). According to the median values, in each period irregular increases in rainfall are expected in winter, between +4% (MT) and +17% (LT) using corrected data and up to 10% (LT) with raw series. In contrast, spring presents slight decreases ranging from -1% to -4% for the corrected data and between -3% and -6% for the raw data. Summer and autumn present irregular fluctuations between ST, MT and LT projections. At annual scale, rainfall anomalies fluctuate over the three future periods and the deviations are always moderate: increases up to +6% according to the median values of bias corrected data, while irregular changes between -4% and +1% for the raw data (median values). It is noteworthy that, the variations between models, in the same period, are higher than the predicted future changes, highlighting the high degree of uncertainty in the results. The effect of downscaling/bias correcting the RCM data is in slightly increasing the range between minimum and maximum anomaly values (the period being equal). The same occurs looking at the interquantile range. According to the RCP 8.5, the anomaly irregularities between seasons and future periods increase (Tab. 4); the variability between models (Fig. 4 and Fig. 5) is higher. With reference to the median values, increments between +3% (ST) and +14% (LT) are expected in winter using the corrected data and up to +10% (LT) with the raw data. In the other seasons, changes are weak but either rising or decreasing. On a yearly scale, changes from -1% to +4% are observed using the corrected data, while reductions between -1% and -5% are obtained with the raw projections.

Similar analyses conducted on precipitation, were adopted to estimate future mean temperature anomalies over the study area. In this case, a temperature anomaly represents the difference (°C) between the future projection and the reference period (RP) data (0 indicates no changes and positive/negative values designate increments/reductions). We used both the downscaled/bias corrected data and the raw ones. Table 5 reports the temperature anomalies at seasonal and annual scale, for each future period (ST, MT and LT) with respect to the RP and according to the RCP 4.5 scenario. With reference to the median values and the

		RCP 4.5 - Corrected data - Temperature Anomaly [-]					RCP 4.5 - Raw data - Temperature Anomaly [-]				
		Winter	Spring	Summer	Fall	Year	Winter	Spring	Summer	Fall	Year
2016-2035	Min	-0.18	-0.03	0.46	0.40	0.42	-0.17	-0.08	0.41	0.40	0.42
	25° perc	0.47	0.57	0.65	0.50	0.63	0.51	0.49	0.60	0.53	0.58
	Median	0.70	0.75	0.84	0.95	0.76	0.84	0.69	0.74	1.03	0.74
	75° perc	0.96	0.97	1.05	1.14	0.94	1.15	0.88	0.97	1.10	0.97
	Max	1.14	1.39	1.31	1.66	1.18	1.22	1.35	1.28	1.79	1.23
2046-2065	Min	0.02	0.72	1.44	0.79	1.04	0.06	0.64	1.21	0.85	0.97
	25° perc	1.12	1.14	1.84	1.36	1.35	1.29	1.01	1.63	1.32	1.30
	Median	1.25	1.34	2.11	1.41	1.52	1.47	1.30	2.12	1.50	1.49
	75° perc	1.41	1.84	2.47	1.70	1.91	1.61	1.71	2.35	1.67	1.94
	Max	2.22	2.37	3.37	2.75	2.47	2.75	2.14	3.84	2.96	2.64
2081-2100	Min	1.07	1.09	1.73	1.53	1.39	1.23	1.00	1.35	1.29	1.22
	25° perc	1.42	1.48	2.02	1.75	1.78	1.70	1.40	1.64	1.78	1.78
	Median	1.86	1.79	2.45	2.07	1.99	2.16	1.47	2.24	2.11	1.96
	75° perc	2.13	2.39	2.93	2.21	2.48	2.38	2.21	2.81	2.33	2.53
	Max	2.76	2.79	3.77	3.30	3.00	3.38	2.52	4.26	3.52	3.16

Tab. 5 - Seasonal and annual temperature anomalies between the reference period (RP, 1986-2005) and the short (ST, 2016-2035), medium (MT, 2046-2065) and long (LT, 2081-2100) term periods, according to the RCP 4.5 scenario and both the downscaled/bias corrected and raw RCM data. The anomalies represent the differences between the future projections and the RP data

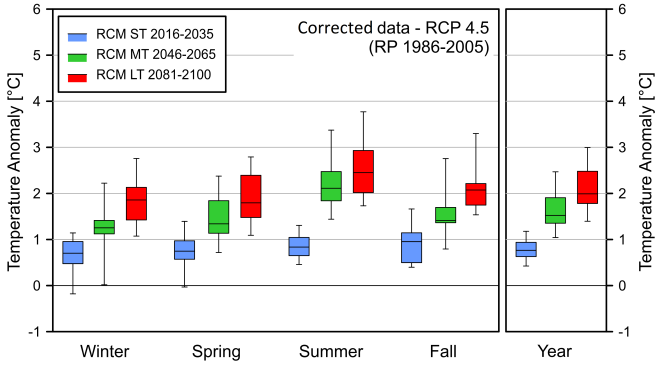

Fig. 6 - Box-whisker plots of the temperature anomalies using the downscaled/bias corrected RCM data at ST, MT and LT, according to the RCP 4.5 scenario. The whiskers extend to the minimum and maximum values

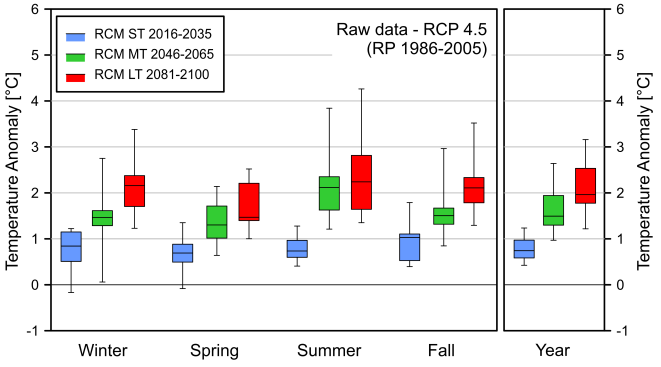

Fig. 7 - Box-whisker plots of the temperature anomalies using the raw RCM data at ST, MT and LT, according to the RCP 4.5 scenario. The whiskers extend to the minimum and maximum values

annual scale we can observe a gradual warming of the study area in the future periods: up to +0.75°C at ST, up to +1.5°C at MT and up to +2°C at LT, using the corrected data. The temperature increments are also visible in Fig. 6 that shows the results in terms of box-whisker plots (the whiskers extend to the maximum and minimum values). Although the increments are evident in each season, these are particularly high in summer. Also using the raw data (Table 5 and Fig. 7), the warming of the study area is unequivocal; similar results are found at annual scale. The effect of the RCM data corrections is in decreasing the range between minimum and maximum anomaly values (the period being equal).

According to the RCP 8.5 (Tab. 6, Fig. 8 and Fig. 9) increments up to +1°C at ST, +2°C at MT and up to +4°C at LT are expected at annual scale; again the higher values are in summer (up to about +5°C, using both raw and corrected data). Even if the warming of the study domain is unequivocal, the results show that, also in the analysis of the future temperature, the variability of the 13 models is wide confirming the high uncertainty of the RCM simulations.

Future seasonal and annual trend analysis

Once identified the future precipitation and temperature anomalies, the RCM data were used to detect the trend evolutions in the climate variables. The analysis is conducted on the time series obtained using a moving time window of thirty years, starting from 1976-2005 and until 2071-2100, advancing one year at a time (a total of 96 overlapping windows). For each time window, both seasonal and annual trends are detected and quantified by means of the Mann-Kendall (MK) test and the method of Theil-Sen (TS), respectively. The climate model data available under the RCP 4.5 and RCP 8.5 scenarios were used in the analysis; for the sake of brevity, only the results obtained using the raw RCM data are presented.

		RCP 8.5 - Corrected data - Temperature Anomaly [-]					RCP 8.5 - Raw data - Temperature Anomaly [-]				
		Winter	Spring	Summer	Fall	Year	Winter	Spring	Summer	Fall	Year
2016-2035	Min	-0.02	0.32	0.58	0.27	0.51	-0.02	0.28	0.57	0.29	0.51
	25° perc	0.56	0.60	0.98	0.81	0.79	0.66	0.54	0.94	0.81	0.73
	Median	0.67	0.84	1.16	0.92	1.00	0.76	0.77	1.18	0.98	0.94
	75° perc	1.13	1.13	1.32	1.17	1.15	1.36	0.97	1.27	1.24	1.18
	Max	1.77	1.56	1.67	1.80	1.53	2.16	1.40	1.37	1.92	1.57
2046-2065	Min	0.45	1.25	1.69	1.75	1.51	0.51	1.25	1.55	1.49	1.45
	25° perc	1.57	1.55	2.35	1.96	1.79	1.68	1.41	1.80	1.97	1.81
	Median	1.81	1.90	2.47	2.07	2.06	2.16	1.82	2.45	2.23	2.09
	75° perc	2.00	2.67	3.36	2.49	2.62	2.28	2.35	3.15	2.63	2.62
	Max	2.45	2.81	3.48	3.29	2.97	3.03	2.69	3.87	3.52	2.95
2081-2100	Min	2.92	2.84	3.67	3.10	3.32	3.13	2.61	3.41	3.26	3.31
	25° perc	3.25	3.35	4.81	3.81	3.89	3.82	3.05	4.18	3.70	3.82
	Median	3.47	3.96	5.13	4.01	4.00	3.96	3.53	5.06	4.29	4.06
	75° perc	3.74	4.78	6.27	4.72	4.91	4.27	4.11	6.03	4.78	5.05
	Max	4.57	5.12	7.04	6.01	5.57	5.62	4.76	7.81	6.45	5.70

Tab. 6 - Seasonal and annual temperature anomalies between the reference period (RP, 1986-2005) and the short (ST, 2016-2035), medium (MT, 2046-2065) and long (LT, 2081-2100) term periods, according to the RCP 8.5 scenario and both the downscaled/bias corrected and raw RCM data. The anomalies represent the differences between the future projections and the RP data

For each of the 96 time windows and the 13 climate models, the presence of trend was evaluated, over the study area, at two significance levels (α): 5% and 10%; the trend gradient was estimated by the TS slope estimator for both the precipitation (mm/year) and temperature (°C/year) time series. In addition, for each window, we evaluated the percentage of models that present a significant trend; we consider meaningful a trend if at least 50% of the 13 models exhibits a significant trend. Following JACOB et alii (2004), in order to detect the robustness of the trends, we calculated the percentage (R) of models (in each time window) that agree in the direction of change; the direction of change was assessed on the basis of the sign of the sum of the MK S-statistics of the 13 RCM models. We consider the trend robust if more than 50% of the models agree in the direction of change.

With reference to the precipitation data, considering the average gradients of the 13 models (ensemble mean), irregular results without significant variations are provided by the RCMs during the entire period. In winter (Fig. 10a), either increasing or decreasing trend have been observed for both scenarios. In Fig. 10, the lighter lines represent the gradients of the single models that show the great variability and associated uncertainty of the results. Also in autumn (Fig. 10b), irregular trend gradients for both scenarios are provided: considering the RCP4.5 (and the ensemble mean) the highest gradient is found in the 2003-2032 period (+1.3 mm/year) and a minimum gradient is obtained (-1.1 mm/year) during the period 2013-2042. Using the RCP 8.5, a maximum of +1.3 mm/year (2032-2061) and a minimum of -1.7 mm/year (2016-2045) is obtained. In summer (Fig. 10c) the variability of the RCMs is more marked; the average of the 13 models is always irregular: a maximum of +1.4 mm/year (2056-2085) and a minimum of -1.7 mm/year (2022-2051) are

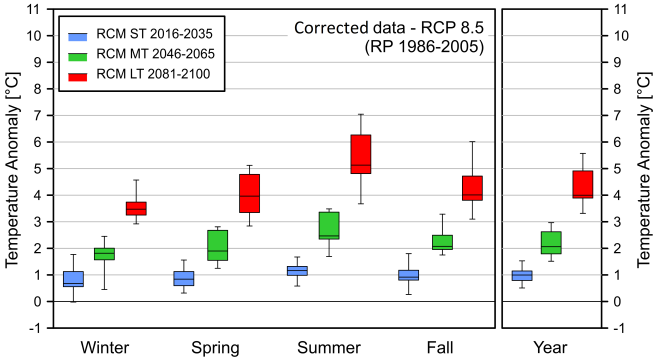

Fig. 8 - Box-whisker plots of the temperature anomalies using the downscaled/bias corrected RCM data at ST, MT and LT, according to the RCP 8.5 scenario. The whiskers extend to the minimum and maximum values

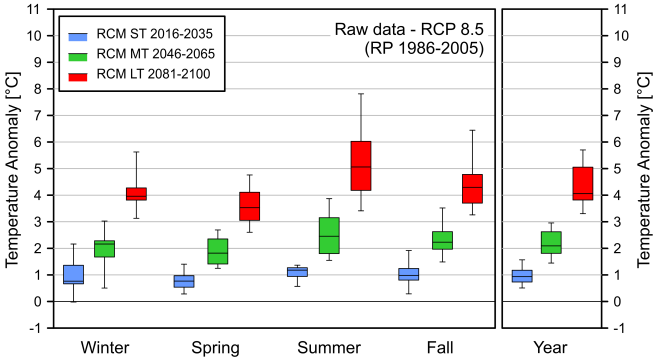

Fig. 9 - Box-whisker plots of the temperature anomalies using the raw RCM data at ST, MT and LT, according to the RCP 8.5 scenario. The whiskers extend to the minimum and maximum values

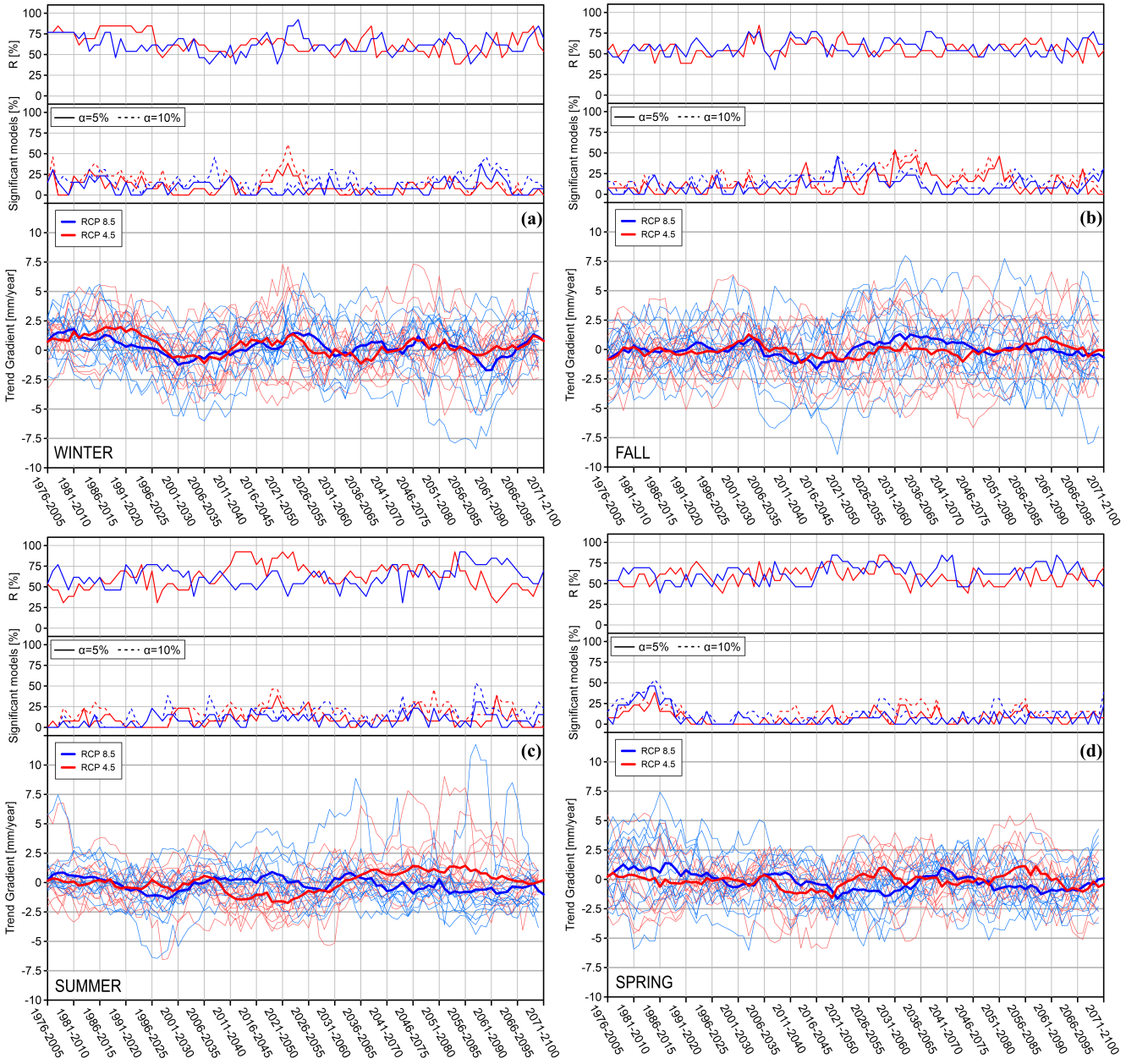

Fig. 10 - Precipitation trend gradient evolution (moving time window of 30 years) at seasonal scale (winter, fall, summer and spring) for both the RCP 4.5 and RCP 8.5 scenarios (bottom plot in each figure). The tick lines represent the mean of the 13 RCMs, the thin lines the single models. Percentage of significant model (central plot in each figure) at the significance level of 5% and 10%; percentage (R) of models that agree in the direction of change (top plot in each figure)

expected with the RCP 4.5, while a maximum of +0.9 mm/year (2019-2048) and a minimum of -1.4 mm/year (2020-2049) are found under the RCP 8.5. In spring (Fig. 10d), considering the RCP 4.5, a maximum gradient of +1.1 mm/year (1999-2028) and a minimum of -1.6 mm/year (2019-2048) are obtained (ensemble mean), while a maximum of +1.4 mm/year (1987-2016) and minimum -1.6 mm/year (2020-2049) are expected with the RCP 8.5. In summary, considering both the scenarios, in each season the variability of the average gradient of the 13 models is always within ± 2.5 mm/year, while with reference to the single models, the variability is much more pronounced but at the same time irregular; the gradients are between +7.5 mm/year and -10.0 mm/year with the exception of the summer, in which the maximum of some models exceeds +10 mm/year.

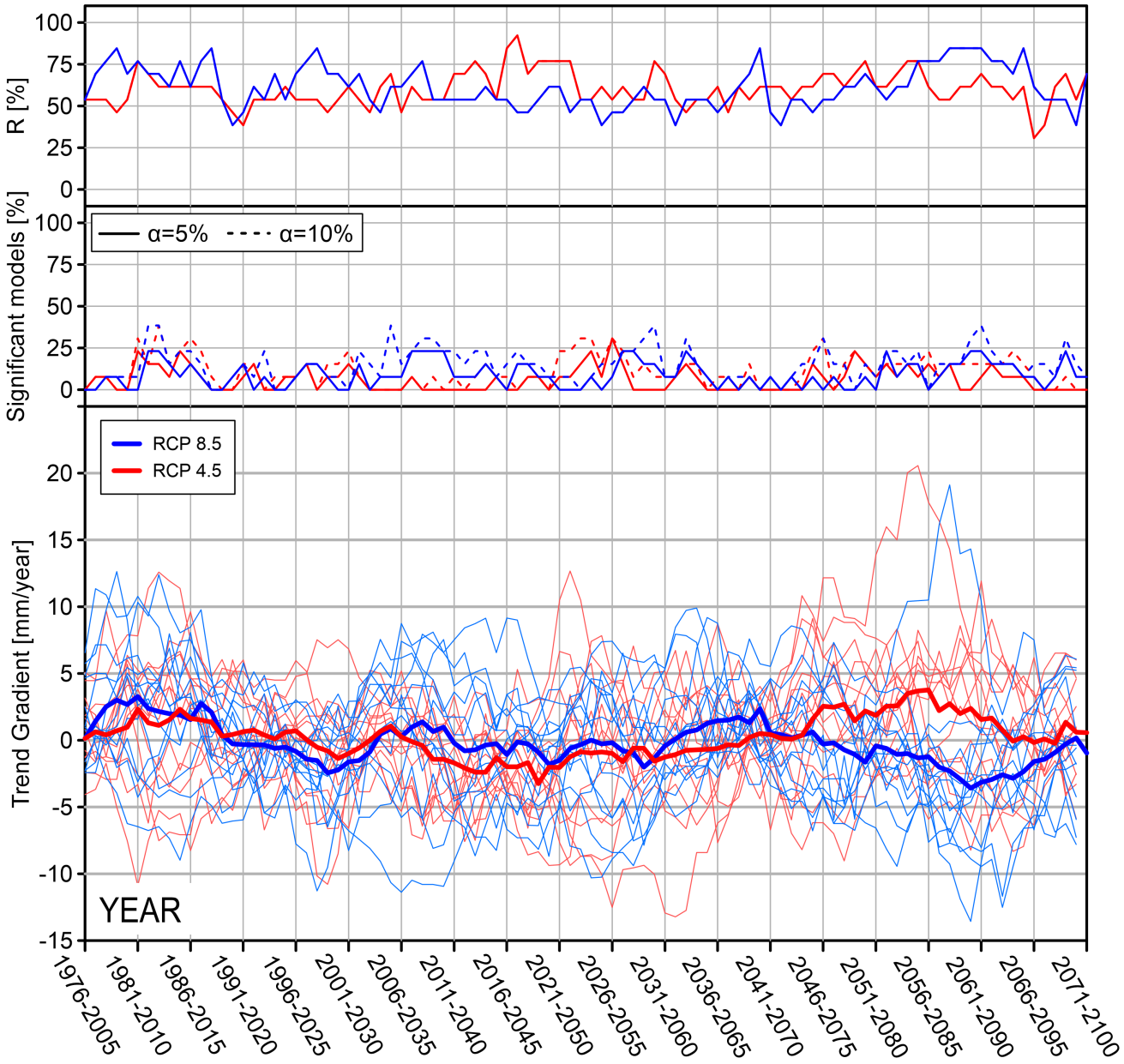

Fig. 11 - Precipitation trend gradient evolution (moving time window of 30 years) at annual scale for both the RCP 4.5 and RCP 8.5 scenarios (bottom plot in each figure). The tick lines represent the mean of the 13 RCMs, the thin lines the single models. Percentage of significant model (central plot in each figure) at the significance level of 5% and 10%; percentage (R) of models that agree in the direction of change (top plot in each figure)

On an annual scale (Fig. 11), the results are consistent with the seasonal ones: the gradients irregularly fluctuate around zero, with a maximum of +3.8 mm/year (2056-2085) and a minimum of -3.2 mm/year (2019-2048), according to the ensemble mean.

According to the MK test, Fig. 10 and Fig. 11 show, at seasonal and annual scale the percentages of the 13 RCM models for which the trend is significant at a level of 5% and 10%. In both cases and scenarios (RCP 4.5 and RCP 8.5), the percentage of significant models results always less than 50%, with few exceptions; we can conclude that the trends are not meaningful. The percentage of models in agreement with the change direction is around 50%; at annual scale there are periods in which the trend can be considered robust.

The analyses on mean temperature show (Fig. 12 and Fig. 13)

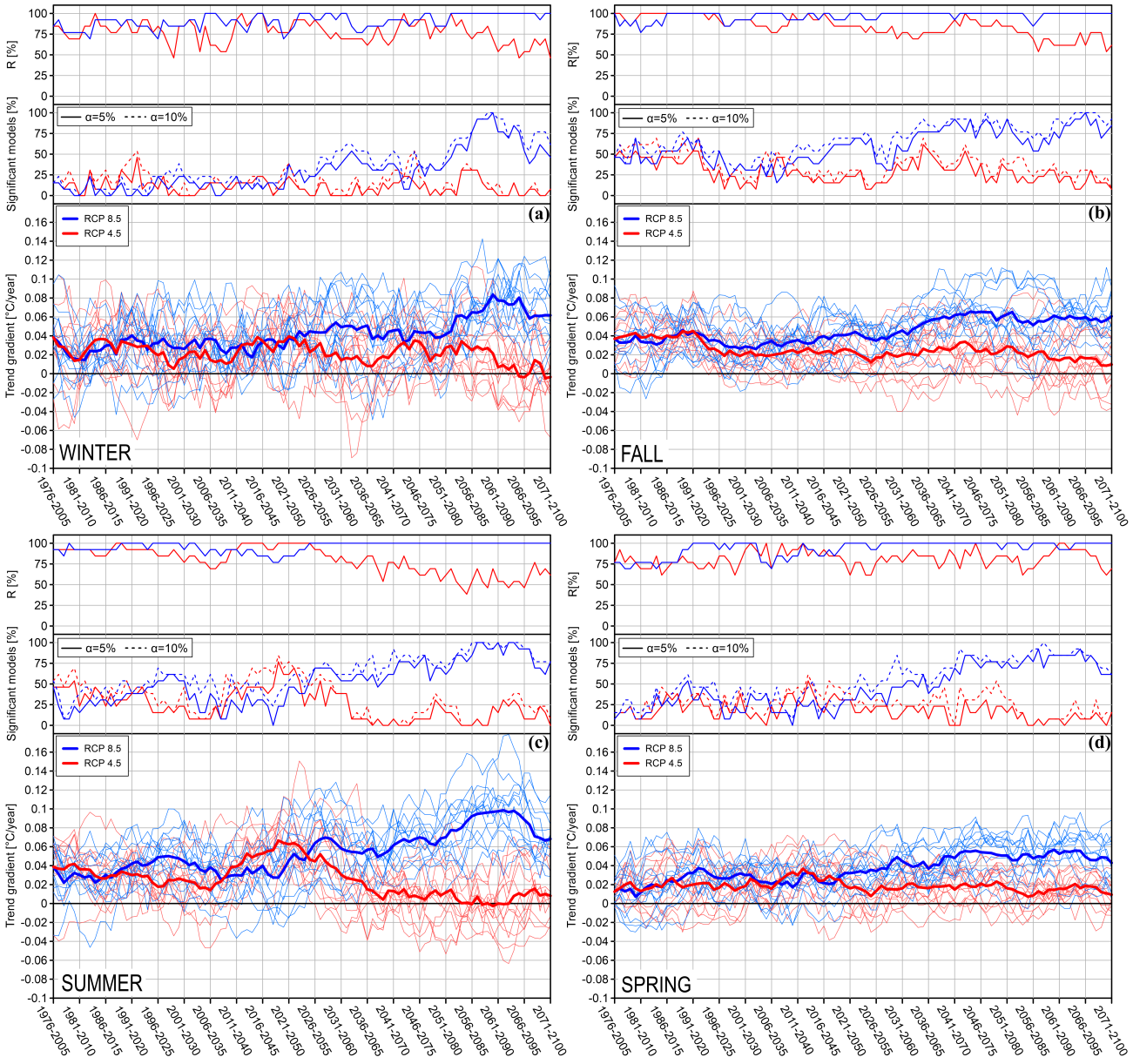

Fig. 12 - Temperature trend gradient evolution (moving time window of 30 years) at seasonal scale (winter, fall, summer and spring) for both the RCP 4.5 and RCP 8.5 scenarios (bottom plot in each figure). The tick lines represent the mean of the 13 RCMs, the thin lines the single models. Percentage of significant model (central plot in each figure) at the significance level of 5% and 10%; percentage (R) of models that agree in the direction of change (top plot in each figure)

trend gradient always positive (according to the ensemble mean) at both seasonal and annual scale, i.e. growing temperature for each time window analyzed (with very few exceptions under the RCP 4.5). In winter (Fig. 12a), the mean trend gradients are substantially the same under the two scenarios until the period 2022-2051 with values ranging from 0 °C/year to 0.04°C/year. After this period, the two curves diverge: under the RCP 4.5, the temperature increases until the end of the century but with lower gradients. In addition, at the end of the century the trends approach zero, which means invariance of temperature. With this scenario, we get the maximum value of +0.04 °C/year in the period 2021-2050. Under the RCP 8.5 the trend gradients are always positive and increase at the end of the century reaching a value of +0.062 °C/year in the period 2071-2100 and a maximum of +0.083 °C/year (2060-2089). However, the trends are non-monotonic over the period but fluctuate both in the median values and, remarkably, in the single model realizations.

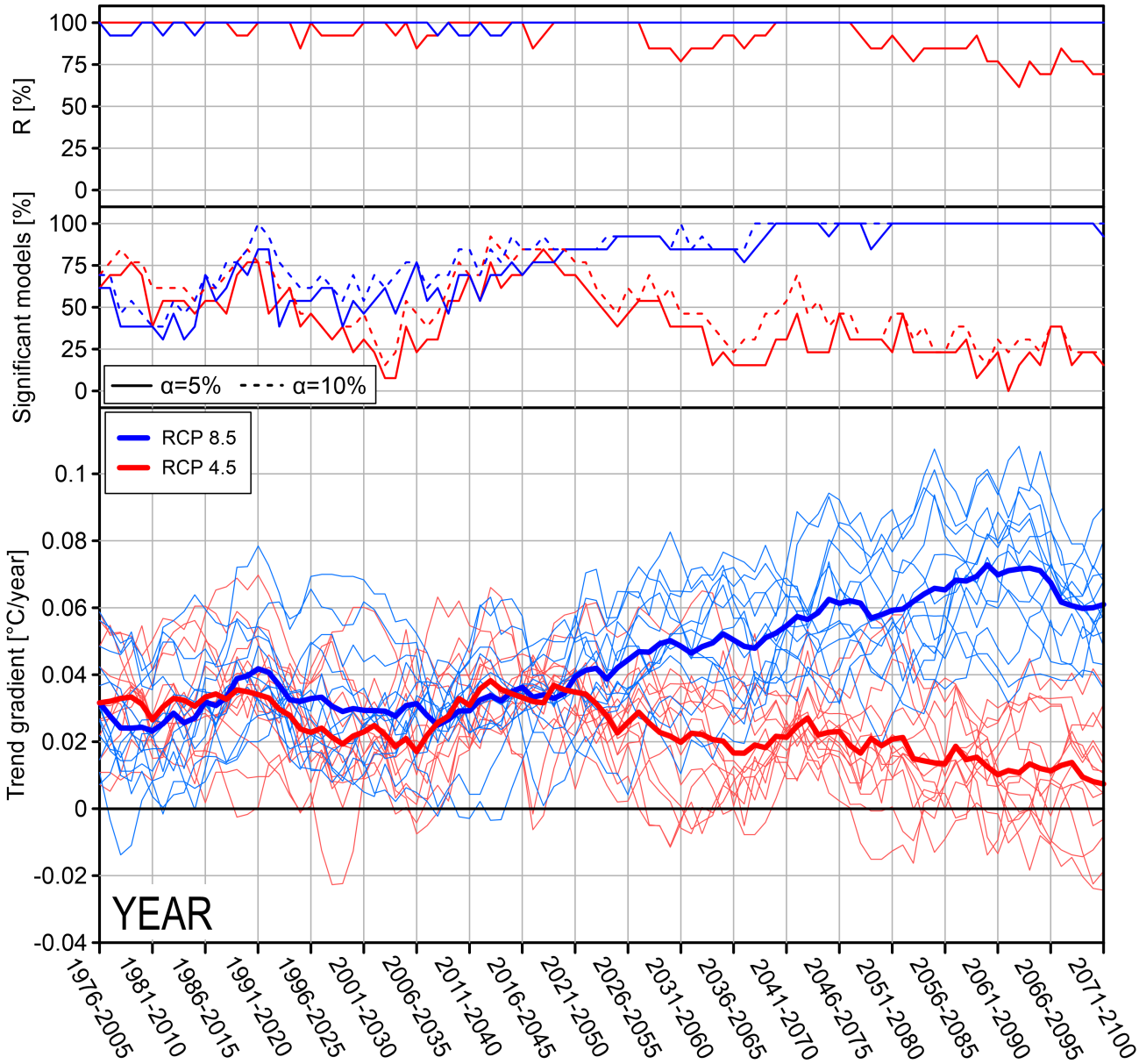

Fig. 13- Temperature trend gradient evolution (moving time window of 30 years) at annual scale for both the RCP 4.5 and RCP 8.5 scenarios (bottom plot in each figure). The tick lines represent the mean of the 13 RCMs, the thin lines the single models. Percentage of significant model (central plot in each figure) at the significance level of 5% and 10%; percentage (R) of models that agree in the direction of change (top plot in each figure)

In fall (Fig. 12b) the trend gradients are always positive and, according to the ensemble mean, the two RCPs present almost the same pattern until the period 1991-2020. Then, under the RCP 4.5, the trend gradient almost stabilizes around 0.02°C/year, while with the RCP 8.5 the trend gradient reaches a value of +0.066 °C/year (2044-2073) and at the end of the century (2071-2100) is +0.061 °C/year. In summer (Fig. 12c) the trend gradients reach the highest values. With the RCP4.5, the maximum gradient of +0.067°C/year is found in the period 2019-2048 (ensemble mean), then the mean trend gradients decrease until the end of the century, reaching a substantial invariance of the temperature (trend gradient of +0.008°C/year) in the period 2071-2100. Under the RCP 8.5, the trend gradient increases over time (with slight oscillations), reaching a maximum of +0.099°C/year in the period 2062-2091; the trend gradient decrease to +0.068°C/year at the end of the century (2071-2100). In spring (Fig. 12d), the trend

evolution reproduces the behavior of autumn, with a maximum of +0.037°C/year in the period 2012-2041 and a subsequent gradient decrease that reaches +0.009°C/year at the end of the century (RCP 4.5). Increasing trends and gradients are found using the RCP 8.5 scenario, with a maximum value of +0.057°C/year just before the end of the century (2060-2089). According to the single models (lighter lines in Fig. 12), a great variability is present in the results with a particular wide range in summer and winter.

At annual scale (Fig. 13), up to the period 2012-2050, the temperature gradients are in the range +0.02 - +0.04°C/year and, according to both the RCPs, do not show substantially differences. Then the trend gradient evolutions diverge; under the RCP 4.5 scenarios, a gradual drop in trend gradients is expected reaching a value of +0.007°C/ at the end of the century (invariance of temperature). With the RCP 8.5, the trend gradient increases over the analyzed period, reaching the maximum in the period 2060-2089 (+0.073°C/year).

The percentage of models with significant trend (Fig. 12 and Fig. 13), at both the 5% and 10% level, is above 50% only for the RCP 8.5 scenario and in the second half of the century. While, at both the seasonal and annual scale, the trends can be considered robust (R above 50% in Fig. 12 and Fig. 13) all over the analyzed time windows, meaning that the majority of models agree in the direction of the changes.

CONCLUSIONS

In this work we analyzed the effect of climate change on the future temperature and precipitation time series over the Taro River, Parma River and Enza River basins. At this aim we made use of an ensemble of 13 RCM projections under two different scenarios (RCP 4.5 and RCP 8.5); both the raw climate model data and the downscaled/bias corrected ones were used. The results, at seasonal and annual scale, show, for both corrected and raw precipitation data, a substantially invariance (irregular positive and negative variations) with changes comparable with the natural variability of the climate. The variability between models is high and so it is the uncertainty of the results. In contrast, the warming of the study area is unequivocal even if the variability of the climate models remains high; the correction of the RCM data decreases the range between minimum and maximum temperature anomalies.

Then we analyzed the trend evolutions in the climate variables using a thirty-year moving time window up to the end of the century. According to the RCP 4.5 scenario, the peak of greenhouse gas concentration is around 2040 then reaching a radiative forcing stabilization to the asymptotic value of 4.5 W/m^2. The RCP 8.5, on the other hand, is characterized by a continuous increase in radiative forcing beyond 2100 (about 8.5 W/m^2 at the end of the century). From the analysis of the future trends, especially for temperature data, it is evident that the pattern of the trend gradients follows the pattern of the scenario radiative forcing. By stabilizing CO_2 concentrations, under the RCP 4.5, a progressive reduction of the temperature increase, that stabilizes at the end of the century, is expected. With the RCP 8.5, on the other hand, concentration levels continue to rise over the century and cause a continuous increase of temperature up to the end of the century. It is noteworthy, that the trend gradients fluctuate over time; for this reason, it is not recommended to extrapolate the investigated climate variable, according to the trend detected in a certain time window, to a larger time horizon.

In the performed analyses, the wide variability of the model projections justifies the use of an ensemble of RCMs that allows accounting for their uncertainty; the use of a single climate model can lead to misleading results.

REFERENCES

Chattopadhyay S. & Edwards D.R. (2016) - *Long term trend analysis of precipitation and air temperature for Kentucky, United States.* Climate, **4** (10). doi: 10.3390/cli4010010.

Chen J., Brissette F.P., Chaumont D. & Braun M. (2013) - *Finding appropriate bias correction methods in downscaling precipitation for hydrologic impact studies over North America.* Water Resources Research, 49, 4187 4205. doi: 10.1002/wrcr.20331

D'Oria M., Ferraresi M. & Tanda M.G. (2017) - *Historical trends and high-resolution future climate projections in northern Tuscany (Italy).* Journal of Hydrology, **555**: 708-723. Doi: 10.1016/j.jhydrol.2017.10.054.

IPCC (2014) - *Climate Change 2014: Synthesis Report. Contribution of Working Groups I, II and III to the Fifth Assessment Report of the Intergovernmental Panel on Climate Change* [Core Writing Team, Pachauri R.K. & Meyer L.A. (Eds.)]. IPCC, Geneva, Switzerland.

Giorgi F., Jones C. & Asrar G.R. (2009) - *Addressing climate information needs at the regional level: the CORDEX framework.* WMO Bulletin, **58**: 175 183.

Gudmundsson L., Bremnes J.B., Haugen J.E. & Engen-Skaugen T. (2012) - *Technical Note: Downscaling RCM precipitation to the station scale using statistical transformations - A comparison of methods.* Hydrol. Earth Syst. Sci., **16**: 3383-3390. Doi: 10.5194/hess-16-3383-2012.

Hamed K.H. (2008) - *Trend detection in hydrologic data: The Mann-Kendall trend test under the scaling hypothesis.* Journal of Hydrology, **349**: 350-363. doi: 10.1016/j.jhydrol.2007.11.009.

Hamed K.H. & Rao A.R. (1998) - *A modified Mann-Kendall trend test for autocorrelated data.* Journal of Hydrology, **204**: 182-196. Doi: 10.1016/S0022-1694(97)00125-X

Jacob D., Petersen J., Eggert B., Alias A., Christensen O.B., Bouwer L.M., Braun A., Colette A., Déqué M., Georgievski G., Georgopoulou E., Gobiet

A., Menut L., Nikulin G., Haensler A., Hempelmann N., Jones C., Keuler K., Kovats S., Kröner N., Kotlarski S., Kriegsmann A., Martin E., Van Meijgaard E., Moseley C., Pfeifer S., Preuschmann S., Radermacher C., Radtke K., Rechid D., Rounsevell M., Samuelsson P., Somot S., Soussana J.-F., Teichmann C., Valentini R., Vautard R. & Weber B., Yiou P. (2014) - *EURO-CORDEX: new high-resolution climate change projections for European impact research.* Regional Environmental Change, **14**: 563-578. Doi: 10.1007/s10113-013-0499-2

Kendall M.G. (1955) - *Rank correlation methods.* Griffin, London.

Mann H.B. (1945) - *Non-parametric tests against trend.* Econometrica, **13**: 163 171.

Nakicenovic N., Alcamo J., Grubler A., Riahi K., Roehrl R.A., Rogner H-H & Victor N. (2000) - *Special Report on Emissions Scenarios (SRES). A Special Report of Working Group III of the Intergovernmental Panel on Climate Change.* Cambridge University Press, Cambridge.

Nalley D., Adamowsli J. & Khalil B. (2012) - *Using discrete wavelet transforms to analyze trends in streamflow and precipitation in Quebec and Ontario (1954-2008).* Journal of Hydrology, **475**: 204-228. Doi: 10.1016/j.jhydrol.2012.09.049.

Razavi T., Switzman H., Arain A. & Coulibaly P. (2016) - *Regional climate change trends and uncertainty analysis using extreme indices: a case study of Hamilton, Canada.* Climate Risk Management, **13**: 43-63.

Semiromi S.T., Moradi H.R., Moghaddam D.D. & Khodagholi M. (2014) - *Future climate conditions and trend analysis of precipitation and temperature in bar watershed, Iran.* Journal of Scientific Research & Reports, **3** (15): 2037-2054.

Sen P.K. (1968) - *Estimates of the regression coefficient based on Kendall's tau*. Journal of the American Statistical Association, **63** (324): 1379-1389.

Sulis M., Paniconi C., Marrocu M., Huard D. & Chaumont D. (2012) - *Hydrologic response to multimodel climate output using a physically based model of groundwater/surface water interactions.* Water Resources Research, **48**.

Teutschbein C. & Seibert J. (2010) - *Regional climate models for hydrological impact studies at the catchment scale: a review of recent modeling strategies*. Geogr. Comp., **4**: 834-860. Doi:10.1111/j.1749-8198.2010.00357.x

Teutschbein C. & Seibert J. (2012) - *Bias correction of regional climate model simulations for hydrological climate-change impact studies: review and evaluation of different methods.* Journal of Hydrology, **456-457**: 12-29. Doi: 0.1016/j.jhydrol.2012.05.052.

Teutschbein C. & Seibert J. (2013) - *Is bias correction of regional climate model (RCM) simulations possible for non-stationary conditions?* Hydrol. Earth Syst. Sci., **17**: 5061-5077. Doi: 10.5194/hess-17-5061-2013

Van Der Liden P., Mitchell J.F.B. & Gilbert P. (2009) - *ENSEMBLES: climate change and its impacts at seasonal, decadal and centennial timescales. Summary of research and results from the ENSEMBLES projects.* Met Office Hadley Centre, Exeter, UK.

Vezzoli R., Mercogliano P., Pecora S., Zollo A.L. & Cacciamani C. (2015) - *Hydrological simulation of Po River (North Italy) discharge under climate change scenarios using the RCM COSMO-CLM.* Science of the Total Environment, **521-522**: 346 358. Doi: 10.1016/j.scitotenv.2015.03.096.

Yue S. & Pilon P. (2004) - *A comparison of the power of the t test, Mann-Kendall and bootstrap tests for trend detection.* Hydrological Sciences, **49** (1).

Received April 2017 - Accepted November 2017